SUPPORTING MATERIAL

In Situ Time-Resolved FRET Reveals Effects of Sarcomere Length on Cardiac Thin-Filament Activation

King-Lun Li[a], Daniel Rieck[a], R. John Solaro[c], Wenji Dong[a, b]

[a]Gene and Linda Voiland School of Chemical Engineering and Bioengineering, Washington State University, Pullman, WA 99164, USA

[b]Integrative Neuroscience and Physiology, Washington State University, Pullman, WA 99164, USA

[c]The Department of Physiology and Biophysics, Center for Cardiovascular Research, College of Medicine, University of Illinois at Chicago, Chicago, IL 60612, USA.

SUPPORTING MATERIALS AND METHODS

Preparation of Proteins

The recombinant double cysteine mutant cTnC(T13C/N51C) from a rat cDNA clone was subcloned into a pET-3d vector, which was then transformed into BL21(DE3) cells (Invitrogen) and expressed under isopropyl β-D-1-thiogalactopyranoside induction. The expressed protein was purified and fluorescently labeled with the FRET donor AEDANS using thiol-reactive 5-(iodoacetamidoethyl)aminonaphthelene-1-sulfonic acid as previously described (1). Unlabeled, singly, and doubly labeled cTnC(T13C/N51C) were separated using a DEAE column. The concentrated singly labeled fraction, $cTnC(T13C/N51C)_{AEDANS}$ (donor-only sample), was collected and divided into two aliquots. One aliquot was subsequently labeled with a large excess of the FRET acceptor DDPM at the other cysteine to obtain the doubly labeled $cTnC(T13C/N51C)_{AEDANS\text{-}DDPM}$ (donor-acceptor sample), and the other aliquot was saved as a reference sample (donor-only sample). The labeling ratio of the donor-only sample was verified to be >95% using UV–vis spectroscopy and the $\varepsilon_{325\ nm}$ of AEDANS, which is 6000 $cm^{-1}\ M^{-1}$.

Animal Handling Protocols

The handling of all the experimental animals followed the institutional guidelines and protocols approved by the Animal Care and Use Committee and the Office of Laboratory Animal Welfare, National Institutes of Health. Our muscle fiber study also followed the established guidelines of and was approved by the Washington State University Institutional Animal Care and Use Committee.

Preparation of pCa Solutions

The reagent concentrations for the pCa (−log of free Ca^{2+} concentration) solutions were calculated based on the program by Fabiato (2). Highly relaxing solution contained the following: 50 BES, 30.83 K-Propionate, 10 NaN_3, 20 EGTA, 6.29 $MgCl_2$, 6.09 Na_2ATP. Maximally activating solution (pCa 4.3) contained the following (in mM): 50 BES, 5 NaN_3, 10 EGTA, 10.11 $CaCl_2$, 6.61 $MgCl_2$, 5.95 Na_2ATP and 51 K-propionate. Relaxing solution (pCa 9.0) had a similar composition (in mM): 50 BES, 5 NaN_3, 10 EGTA, 0.024 $CaCl_2$, 6.87 $MgCl_2$, 5.83 Na_2ATP and 71.14 K-propionate. For crossbridge inhibiting solution, 1 mM sodium Vi was added to the above pCa solutions. For ADP-mediated non-cycling, strong-binding cross-bridge solutions, ATP was removed from relaxing and maximally activating solutions, and 5 mM Mg^{2+}-ADP was added in its place. The ionic strength of all pCa solutions was 180 mM. In addition, protease inhibitors including 5 μM bestatin, 2 μM E-64, 10 μM leupeptin, and 1 μM pepstatin were also added to the pCa solutions (3).

Preparation of Detergent-Skinned Cardiac Muscle Fibers

Left ventricular papillary bundles from adult (6–8 months in age) Long–Evans rats were prepared using protocol established by Chandra and coworkers (4). Animals were deeply anesthetized by inhalation of isoflurane and hearts were quickly excised and placed into ice-cold highly relaxing solution that contained the following: 50 mM N,N-bis (2-hydroxyethyl)-2-aminoethane-sulfonic acid (BES), pH 7.0, 30.83 mM K propionate, 10 mM Na azide, 20 mM ethylene glycol tetraacetic acid (EGTA), 6.29 mM $MgCl_2$, 6.09 mM Na_2ATP, 1.0 mM DTT, and 20 mM 2,3-butanedione monoxime. A fresh protease inhibitors including 4 μM benzamidine-HCl, 5 μM bestatin, 2 μM E-64, 10 μM leupeptin, 1 μM pepstatin and 200 μM phenylmethylsulfonyl fluoride were added to the solution. Papillary muscle bundles were carefully removed from the left ventricles of rat hearts. Muscle fibers (~150–200 μm in diameter and 2.0 mm in length) were dissected and skinned overnight at 4 °C using 1% triton X-100 in highly relaxing solution.

Reconstitution of detergent-skinned, cTnC-extracted rat myocardial fibers with modified cTnC

Incorporation of modified cTnC into cardiac muscle fibers was based on a extraction/reconstitution method described previously (1). Endogenous cTnC in detergent-skinned rat cardiac muscle fibers was first removed by incubating fibers in an extraction solution for 2.5-3 hours. The extraction solution contained (in mM): 5 trans-1,2-cyclohexanediamine-N,N,N',N'-tetraacetic acid (CDTA), 40 Tris-HCl (pH 8.4.), 0.6 NaN_3, 0.005 bestatin, 0.002 E-64, 0.01 leupeptin, and 0.001 pepstatin. cTnC-extracted fibers were washed with the relaxing solution and then incubated overnight in cTnC solution (1.5 mg mL^{-1}) containing either donor-only or donor-acceptor modified cTnC(T13C/N51C) in the presence of myosin light chain-2 (0.76 mg mL^{-1}). Ca^{2+}-

activated maximal tension was measured in pCa 4.3 solution for cTnC-depleted fibers to determine the residual tension and for exogenous cTnC reconstituted fibers to determine recovery of maximum tension.

SDS–PAGE and Western blotting analysis of reconstitution levels of modified cTnC in cardiac muscle

Based on previously described methods (1), detergent-skinned cardiac muscle fibers reconstituted with modified cTnC were incubated in 10 μL of a protein extraction buffer per 1 muscle fiber on ice for 1 hr. Skinned fibers that had not undergone extraction were similarly incubated to create a negative control. The protein extraction buffer contained 2.5% SDS, 10% glycerol, 50 mM Tris base (pH 6.8 at 4 °C), 1 mM DTT, 1 mM phenylmethylsulfonyl fluoride, 4 mM benzamidine HCl, 5 μM bestatin, 2 μM E-64, 10 μM leupeptin, and 1 μM pepstatin. After incubation, samples were sonicated for 20 min in a water bath at 4 °C and centrifuged at 10k rpm. The supernatants were loaded to SDS–PAGE gels for Western blotting analysis. Sample loading amounts were standardized between each sample by estimating total protein concentration and further optimized based on relative actin concentrations. Equal amounts of protein were loaded and separated on a 4–20% SDS–PAGE gel. Separated proteins were then transferred to polyvinylidene difluoride membrane. The membrane was incubated in a blocking solution containing Tris-buffered saline with 2% tween-20 (TBS/T) and 5% dry milk. The blocked membrane was then treated with 1:5000 dilution of primary mouse anti-rat antibody against cTnC (Fitzgerald 10-T78A) in blocking solution overnight. Excess primary antibody was successively rinsed away by washing the membrane several times with TBS/T. The primary antibody treated membrane was further treated with 1:5000 dilution of horseradish peroxidase conjugated sheep anti-mouse antibody (Amersham NTF825) in blocking solution for 1 hour. An enhanced luminol-based chemiluminescent (ECL) kits (Amersham ECL Western Blotting Analysis System RPN 2108) was then used to detect the level of cTnC in the fiber samples.

Experimental Apparatus

A previously described Güth muscle research system (1) was used in this study to simultaneously make biomechanical and optical measurements. Isometric force measurements were conducted using a force transducer (SI Heidelberg KG7A) capable of measuring 5 mN with a resonance frequency of 500 Hz. Detergent-skinned left ventricular cardiac muscle fiber samples from normal adult male Long–Evans rats were mounted between the force transducer and a stationary tweezer. A quartz perfusion cuvette with a diameter of 1 mm was slipped over the preparation and pCa solution was continuously perfused through the mounted fiber during experimentation. The SL of the fiber was adjusted to either 1.8 or 2.2 μm using He-Ne laser diffraction measurements. The temperature of the pCa solution within the cuvette was held a 20 ± 0.2 °C using a bipolar temperature controller (Cell MicroControls TC2BIP) coupled with a cooling/heating module (Cell MicroControls CH). To perform time-resolved fluorescence measurements with chemically skinned muscle fibers containing modified cTnC, the MRS was modified by replacing the photomultiplier tube in its PH1A microscope photometer with a TBX picosecond photon detection module (HORIBA Jobin Yvon). To eliminate uncontrolled factors that can affect the conformational state of N-cTnC during rising phase of force development, time-resolved fluorescence measurements were made when fiber force reached steady-state (Fig. 1B). Excitation light at 340 nm was projected onto the muscle fiber through the cuvette from a NanoLED (HORIBA Jobin Yvon N-340) with a <1.2 ns pulse width. The total fluorescence emission from the central area of the muscle fiber was isolated for measurement using the PH1A microscope window slit and optics to focus the light onto the TBX, and fluorescence intensity decays of muscle fibers containing either donor-only or donor-acceptor modified cTnC(T13C/N51C) were processed and recorded by a FluoroHub-B (HORIBA Jobin Yvon). With this instrument setup, a total of 10,000 photon counts at peak channel for each decay collection was achieved in 1–1.5 min.

Simultaneous Measurement of Isometric Force and Time-Resolved Fluorescence Intensity in Detergent-Skinned Cardiac Muscle Fibers

To eliminate experimental uncertainty from variations in handling between fiber preparations, isometric force and time-resolved fluorescence measurements were observed at both 1.8 and 2.2 μm SLs with the same muscle fiber according to the following measurement protocol. SL was adjusted to either 1.8 or 2.2 μm SL using laser diffraction and subjected to an initial cycle of activation and relaxation, after which the SL was readjusted if necessary. Half of our measurements were started at 1.8 μm SL, whereas the other half was started at 2.2 μm SL. Isometric force and a fluorescence intensity decay were then synchronously, digitally recorded as the fiber was subjected to pCa 4.3 solution at the chosen SL. After completion of the measurement, highly relaxing solution, containing 20 mM EGTA, was used to completely relax the fiber, and then force and an intensity decay were recorded. The SL of the fiber was then adjusted to the opposite SL of the one that was initially chosen; for example, if the measurement had started with 1.8 μm SL, then the fiber was adjusted to a SL of 2.2 μm. Recordings were then made with pCa 4.3 and pCa 9.0 solutions in the same fashion as before. The order with which SLs were tested was

later found to exert no discernable effect on the outcome of experiments. This same measurement protocol was used to perform tr-FRET measurements of N-cTnC opening in the presence of cycling cross-bridges (5 mM Mg-ATP); Mg^{2+}-ADP-induced non-cycling, strong-binding cross-bridges (5 mM Mg-ADP + 0 mM ATP); and vanadate-induced non-cycling, weak-binding cross-bridges (1 mM Vi + 5 mM Mg-ATP).

There are some important experimental design considerations for using Vi to inhibit strong cross-bridge binding, which are as follows. Myosin can be UV photocleaved by the tetrameric form of aqueous Vi (5-7), but photocleavage kinetics are greatly attenuated by the presence of ATP and actin (8) such that photocleavage is not a concern on the timescales involved in our experiments here. This was confirmed here by the fact that following the tr-FRET measurement protocol, maximal force could be recovered on average to 88.0 ± 2.3% regardless of test condition. Furthermore, when higher Vi concentrations are used (~10 mM), polymeric species of vanadate becomes significantly present in solution, and it is this polymeric species of vanadate that has been implicated as extracting cTnI and cTnC from the troponin complex (9). Because of our lower concentration of Vi at 1 mM, no extraction of cTnI and cTnC was expected. Confirming this, no significant change in passive tension at pCa 9 was observed following the tr-FRET measurement protocol conducted in the presence of Vi, indicating that no appreciable Vi-mediated extraction of cTnI and cTnC had occurred.

Determination of Inter-Probe Distance Distrubutions from Measured Fluorescence Intensity Decays

The AEDANS-DDPM inter-probe distance distribution associated with a specific test condition was determined as follows. The AEDANS excited-state decays observed for the donor-only samples were fitted with a multi-exponential function (10):

$$I_D(t) = \sum_{i=1}^{n} \alpha_i \, e^{-t\,\tau_i^{-1}} \tag{S1}$$

where the α_i represents the fractional amplitude associated with each correlation time τ_i contributing that contributes to the overall excited-state decay process. In the presence of the non-fluorescent acceptor DDPM, the AEDANS excited-state decays observed for donor−acceptor samples were fit to the following equation using GlobalCurve analysis software (11):

$$I_{DA}(t) = \frac{\int_0^{\infty} P(r)\left(\sum_{i=1}^{n} \alpha_{D_i} \, e^{-\frac{t}{\tau_{D_i}}\left(1+\left(\frac{R_0}{r}\right)^6\right)}\right) dr}{\int_0^{\infty} P(r)\, dr} \tag{S2}$$

where r is the distance between the donor and acceptor fluorophores; α_{Di} and τ_{Di} are the fractional amplitude and correlation time parameters, respectively, determined for AEDANS in the absence of DDPM; and R_o is the Förster critical distance at which energy transfer is 50% efficient. $P(r)$ is the probability distribution of inter-probe distances, and in this study we assume it to be a single Gaussian as follows:

$$P(r) = \frac{1}{Z\,\sigma\sqrt{2\pi}} e^{-\frac{1}{2}\left(\frac{r-\bar{r}}{\sigma}\right)^2} \tag{S3}$$

where r is the mean distance and σ is the standard deviation of the distribution. $P(r)$ is normalized by area, and Z is the normalization factor. The half width at half maximum (*HWHM*) of the distribution is given by $HWHM = 1.1772\sigma$. In practice, the integration limits in Eq. 3 are not from 0 to ∞, and the integral is instead calculated over a range of distances from r_{min} to r_{max} with the lower limit being about 5 Å.

The Förster distance R_o in Eq. 2 was calculated from the spectral properties of AEDANS and DDPM:

$$R_0 = (8.79\times10^{-5}) n^{-4} Q \kappa^2 J \tag{S4}$$

where n is the refractive index of the solution and was taken as 1.4, Q is the donor quantum yield, κ^2 is the orientation factor, and J is the spectral overlap integral that is given by

$$J = \frac{\int F_D(\lambda)\,\varepsilon_A(\lambda)\,\lambda^4\, d\lambda}{\int F_D(\lambda)\, d\lambda} \tag{S5}$$

where $F_D(\lambda)$ is the fluorescence intensity of the donor at wavelength λ and $\varepsilon_A(\lambda)$ is the molar absorptivity of the acceptor at λ. J was calculated by numerical integration. Dynamic averaging and the associated value of ⅔ for κ^2 were assumed, which is valid when donor and acceptor probes tumble rapidly and randomly over the course of the measurement, which is a condition that we expected since the Cys-13 and Cys-51 of cTnC are located in surface-exposed loops. To ensure that the average orientations of the probes attached to Cys-13 and Cys-51 did not change significantly between different test conditions, which would result in unknown changes in κ^2 between conditions, the potential for a change in κ^2 was assessed by measuring the anisotropy of AEDANS under each test condition (12) (see below). The contribution of potential differences in κ^2 to changes in FRET efficiency between different states was found to be minimal (Fig. S1).

Measurement of *In Situ* Fluorescence Anisotropy

Time-resolved fluorescence anisotropy measurements were performed on chemically skinned, cTnC-extracted muscle fibers reconstituted with $cTnC(T13C/N51C)_{AEDANS}$. Because DDPM is non-fluorescent, its orientation within the muscle fiber could not be assessed using anisotropy measurements. However, our labeling scheme results in a random attachment of AEDANS to either Cys-13 or Cys-51 in $cTnC(T13C/N51C)_{AEDENS}$, so it is

likely that AEDENS anisotropies observed in donor-only samples are a good representative of probe orientation within $cTnC(T13C/N51C)_{AEDENS/DDPM}$. To measure AEDANS time-resolved anisotropy decays, the MRS was first modified by placing a pair of optical polarizers within the excitation and emission light paths. To collect time-resolved fluorescence anisotropy decays, upon excitation with vertically polarized 340 nm light oriented along axis of the fiber, vertically and horizontally polarized emissions of 480 nm from the reconstituted muscle fibers were recorded separately by manually changing orientation of the emission polarizer every 4 min with a total of 16 min of data collection. Each set of total fluorescence intensity decays was combined to generate a time-resolved anisotropy decay using anisotropy analysis software provide by HORIBA Jobin Yvon. The same software was used to fit the anisotropy decays to the following equation (10,13):

$$r_{anis} = r_0 \sum_{i=1}^{n} \alpha_i \, e^{-t \Phi_i^{-1}} \qquad \text{(S6)}$$

where r_0 is the limiting anisotropy and α_i is the fractional amplitude of each correlation time (Φ_i) that contributes to the overall anisotropy decay. Results are shown in Fig. S2.

SUPPORTING REFERENCES

1. Rieck, D. C., K.-L. Li, Y. Ouyang, R. J. Solaro, and W.-J. Dong. 2013. Structural basis for the in situ Ca^{2+} sensitization of cardiac troponin C by positive feedback from force-generating myosin cross-bridges. *Arch. Biochem. Biophys.* 537:198-209.
2. Fabiato, A., and F. Fabiato. 1979. Calculator programs for computing the composition of the solutions containing multiple metals and ligands used for experiments in skinned muscle cells. *J. Physiol. (Paris)* 75:463-505.
3. Chandra, M., M. L. Tschirgi, S. J. Ford, B. K. Slinker, and K. B. Campbell. 2007. Interaction between myosin heavy chain and troponin isoforms modulate cardiac myofiber contractile dynamics. *Am. J. Physiol.* 293:R1595-1607.
4. Ford, S. J., R. Mamidi, J. Jimenez, J. C. Tardiff, and M. Chandra. 2012. Effects of R92 mutations in mouse cardiac troponin T are influenced by changes in myosin heavy chain isoform. *J. Mol. Cell. Cardiol.* 53:542-551.
5. Grammer, J. C., C. R. Cremo, and R. G. Yount. 1988. UV-induced vanadate-dependent modification and cleavage of skeletal myosin subfragment 1 heavy chain. 1. Evidence for active site modification. *Biochemistry* 27:8408-8415.
6. Mocz, G. 1989. Vanadate-mediated photocleavage of rabbit skeletal myosin. *Eur. J. Biochem.* 179:373-378.
7. Cremo, C. R., G. T. Long, and J. C. Grammer. 1990. Photocleavage of myosin subfragment 1 by vanadate. *Biochemistry* 29:7982-7990.
8. Muhlrad, A., Y. M. Peyser, and I. Ringel. 1991. Effect of actin, ATP, phosphates, and pH on vanadate-induced photocleavage of myosin subfragment 1. *Biochemistry* 30:958-965.
9. Strauss, J. D., C. Zeugner, J. E. Van Eyk, C. Bletz, M. Troschka, and J. C. Rüegg. 1992. Troponin replacement in permeabilized cardiac muscle reversible extraction of troponin I by incubation with vanadate. *FEBS Lett.* 310:229-234.
10. Liao, R., C. K. Wang, and H. C. Cheung. 1992. Time-resolved tryptophan emission study of cardiac troponin I. *Biophys. J.* 63:986-995.
11. Dong, W.-J., J. R. Robinson, E. C.-Y. Lin, B. Ruzsics, J. Xing, and H. C. Cheung. 2004. Ca^{2+}-induced opening of the N-domain of cTnC in regulated cardiac thin filament. *Biophys. J.* 86:396a.
12. Dale, R. E., J. Eisinger, and W. E. Blumberg. 1979. The orientational freedom of molecular probes. The orientation factor in intramolecular energy transfer. *Biophys. J.* 26:161-193.
13. Zhou, Z., K.-L. Li, D. Rieck, Y. Ouyang, M. Chandra, and W.-J. Dong. 2012. Structural dynamics of C-domain of cardiac troponin I protein in reconstituted thin filament. *J. Biol. Chem.* 287:7661-7674.

Table S1: Cys-13–Cys-51 distance distributions observed in cTnC(N13C/T51C)$_{AEDANS-DDPM}$-reconstituted fibers under different biochemical conditions. Normalized parameter values are shown and given as mean ± SEM.

Cross-bridge state	pCa	Normalized *r* [a]		Normalized *HWHM* [b]	
		1.8 μm SL	2.2 μm SL	1.8 μm SL	2.2 μm SL
5 mM ATP	9.0	0.09 ± 0.03	0.00 ± 0.04	0.84 ± 0.09	0.97 ± 0.01
	4.3	0.79 ± 0.05	1.00 ± 0.03	0.74 ± 0.06	1.08 ± 0.05
1 mM Vi[c]	9.0	−0.01 ± 0.01	−0.06 ± 0.01	0.69 ± 0.08	0.74 ± 0.03
	4.3	0.60 ± 0.05	0.58 ± 0.04	0.69 ± 0.04	0.79 ± 0.04
5 mM ADP[d]	9.0	0.02 ± 0.05	0.16 ± 0.02	0.77 ± 0.06	0.59 ± 0.03
	4.3	0.84 ± 0.02	1.11 ± 0.01	0.74 ± 0.08	0.51 ± 0.10
0.5 mM Vi[c]	9.0	–	0.03 ± 0.02	–	0.88 ± 0.02
	4.3	–	0.87 ± 0.02	–	0.73 ± 0.06
2.5 mM ADP[d]	9.0	–	0.12 ± 0.03	–	0.70 ± 0.01
	4.3	–	1.04 ± 0.03	–	0.86 ± 0.05

[a] *r* is the mean distance associated with the distribution (see Eq. 3). Normalized values were calculated by taking the absolute *r* value observed under 5 mM ATP, pCa 9, and 2.2 μm SL as "0"; whereas "1" was taken as the absolute *r* value observed under 5 mM ATP, pCa 4.3, and 2.2 μm SL.

[b] *HWHM* denotes the half width at half maximum (see Eq. 3 and following text). Normalized *HWHM* values were determined according to the equation: $HWHM_{norm} = HWHM_{raw} / (r_{max} - r_{min})$. The value of r_{max} was taken as 32.97 from the pCa 4.3 + 5 mM ATP + 2.2 μm SL condition (see Table 1 of main text), whereas the value of r_{min} was taken as 25.53 from the pCa 9 + 5 mM ATP + 2.2 μm SL condition.

[c] Vi solutions also contained 5 mM ATP.

[d] ATP was absent in ADP solutions.

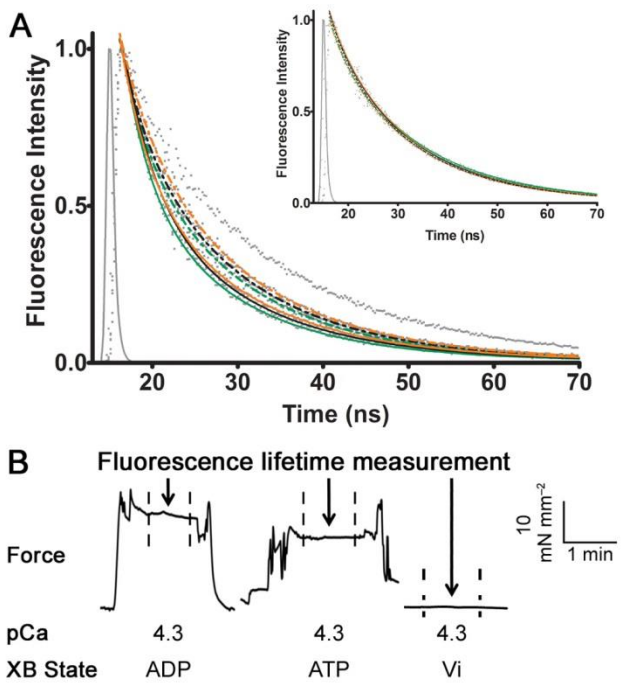

Figure S1. Representative traces of simultaneously recorded isometric force and total fluorescence intensity decay from skinned rat left ventricular papillary muscle reconstituted with either cTnC(T13C/N51C)$_{AEDANS}$ or cTnC(T13C/N51C)$_{AEDANS\text{-}DDPM}$. Measurements were taken at a SL of 2.2 µm and pCa 9 and pCa 4.3 under the biochemical conditions indicated below the force trace in panel B. (A) *Gray dots* are used to plot each raw intensity decay profile. In the main panel, *lines* represent fittings of Eqn. 1 to raw decay profiles and also indicate traces for fibers reconstituted with cTnC(T13C/N51C)$_{AEDANS\text{-}DDPM}$. *Solid lines* and *dashed lines* indicate measurements taken at pCa 9 and pCa 4.3, respectively. *Green lines*, *orange lines*, and *black lines* indicate that fibers were treated with 1 mM Vi, 5 mM ADP-Mg, or 6.13 mM ATP, respectively. The *inset* graph shows traces and fittings for cTnC(T13C/N51C)$_{AEDANS}$ fibers tested under the same conditions. (B) Arrows and dashed lines indicate how fluorescence intensity decays were measured when active force had reached steady state. Force and time magnitudes are indicated by the horizontal and vertical bars. The maximal active force developed by cTnC(T13C/N51C)$_{AEDANS\text{-}DDPM}$-reconstituted fibers was 25.6 ± 1.8 mN mm^{-2}, which was not significantly different from the 28.4 ± 3.6 mN mm^{-2} maximal active force developed by cTnC(wt)-reconstituted fibers (p = 0.1192).

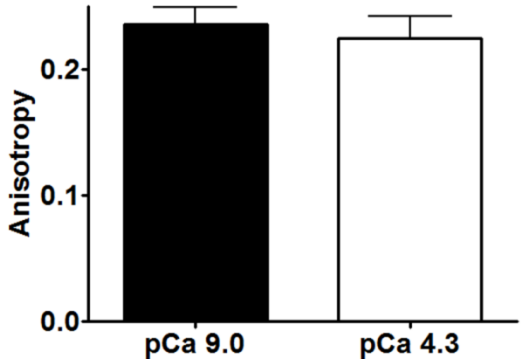

Figure S2: Anisotropy of cTnC(13C/51C)$_{AEDANS-DDPM}$ measured *in situ* under conditions of normal cross-bridge cycling.

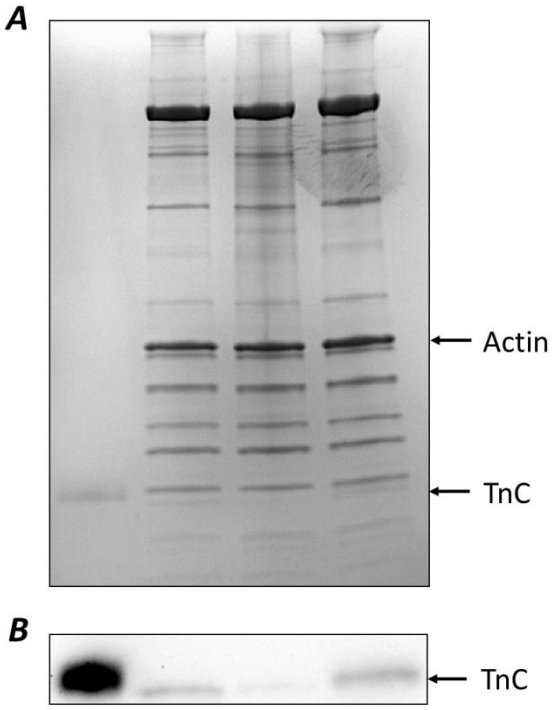

Figure S3. Assessment of cTnC incorporation in reconstituted muscle fibers. Starting from the left, *lane* 1 represents purified recombinant cTnC(wt). *Lane* 2, 3, and 4 indicate samples from skinned, CDTA treated, and cTnC(13C/N51C)$_{\text{AEDENS-DDPM}}$ reconstituted muscle fibers, respectively. (A) Coomassie blue stain was used to reveal the total protein content in the SDS-PAGE gel. (B) Anti-cTnC antibody was used to assess the extents of endogenous cTnC extraction and cTnC(13C/N51C)$_{\text{AEDENS-DDPM}}$ incorporation into reconstituted fibers. Image J software was used to analyze the protein band intensities in lane 2 to 4.

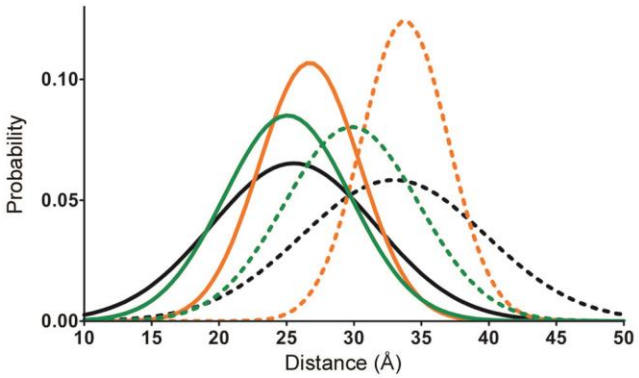

Figure S4. Area normalized versions of the N-cTnC Cys-13–Cys-51 distance distributions observed at 2.2 µm SL and shown in Fig. 1B of the main text. Conditions are as follows: pCa 9 + ATP (*black solid line*), pCa 4.3 + ATP (*black dotted line*), pCa 9 + ADP (*orange solid line*), pCa 4.3 + ADP (*orange dotted line*), pCa 9 + Vi (*green solid line*), and pCa 4.3 + Vi (*green dotted line*).

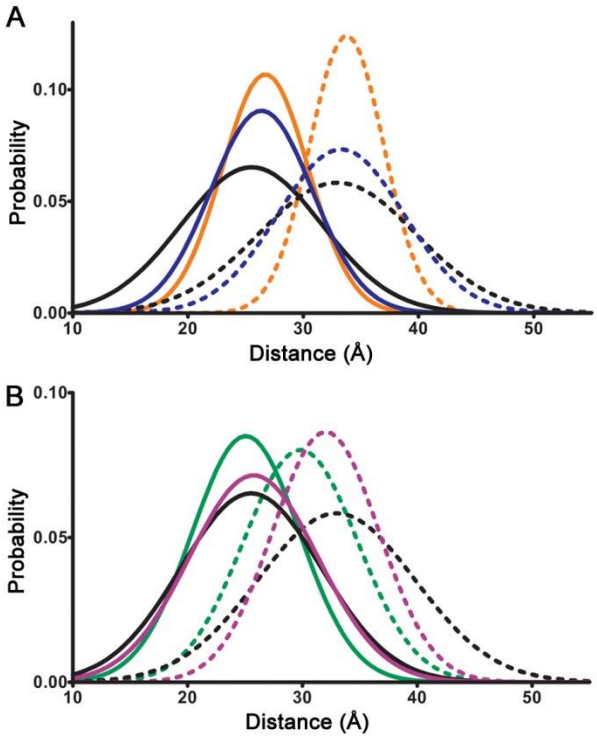

Figure S5. Area normalized versions of the N-cTnC Cys-13–Cys-51 distance distributions shown in Fig. 2 of the main text, which were observed at 2.2 µm SL under intermediate and saturating concentrations of ADP and Vi. (A) Conditions are as follows: pCa 9 + ATP (*black solid line*), pCa 4.3 + ATP (*black dotted line*), pCa 9 + 2.5 mM ADP (*blue solid line*), pCa 4.3 + 2.5 mM ADP (*blue dotted line*), pCa 9 + 5 mM ADP (*orange solid line*), and pCa 4.3 + 5 mM ADP (*orange dotted line*). (B) Conditions are: pCa 9 + ATP (*black solid line*), pCa 4.3 + ATP (*black dotted line*), pCa 9 + 0.5 mM Vi + ATP (*purple solid line*), pCa 4.3 + 0.5 mM Vi + ATP (*purple dotted line*), pCa 9 + 1 mM Vi + ATP (*green solid line*), and pCa 4.3 + 1 mM Vi + ATP (*green dotted line*).

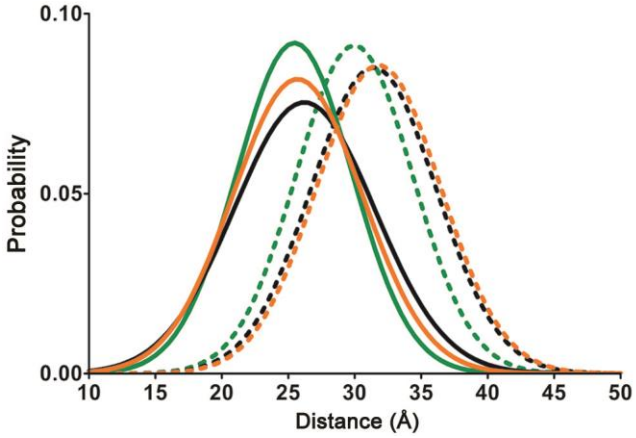

Figure S6. Area normalized versions of the N-cTnC Cys-13–Cys-51 distance distributions observed at 1.8 µm SL and shown in Fig. 5A of the main text. Conditions are as follows: pCa 9 + ATP (*black solid line*), pCa 4.3 + ATP (*black dotted line*), pCa 9 + ADP (*orange solid line*), pCa 4.3 + ADP (*orange dotted line*), pCa 9 + Vi (*green solid line*), and pCa 4.3 + Vi (*green dotted line*).